J. Anat. (1986), **147**, pp. 55–72
With 18 *figures*
Printed in Great Britain

A quantitative ultrastructural comparison of alpha and gamma motoneurons in the thoracic region of the spinal cord of the adult cat

IAN P. JOHNSON

Sobell Department of Neurophysiology, Institute of Neurology, Queen Square, London WC1N 3BG

(*Accepted* 7 *October* 1985)

INTRODUCTION

The ventral horn of the spinal cord contains neuronal cell bodies of various sizes (Sprague, 1951; Rexed, 1952), of which two classes can be distinguished: motoneurons and interneurons. Under appropriate conditions, almost all the cell bodies of large diameter exhibit retrograde chromatolysis following peripheral nerve section and they are therefore considered to be motoneurons. Of the small diameter cell bodies, however, only 10–15 % exhibit chromatolysis under similar circumstances, leaving the identity of the remaining small neurons uncertain because of the vagaries of the chromatolytic method (Schadé & Van Harreveld, 1961; Nyberg-Hansen, 1965; Romanes, 1964).

There are numerous light and electron microscopic studies of large motoneurons. In contrast, there are very few anatomical descriptions of small motoneurons and these have been restricted to light microscopy (Bryan, Trevino & Willis, 1972; Strick *et al.* 1976; Westbury, 1979; Ulfhake & Cullheim, 1981).

In the present study, a quantitative ultrastructural comparison of large and small motoneurons in the thoracic spinal cord of the cat has been undertaken using horseradish peroxidase as a retrograde neuronal marker to distinguish motoneurons from interneurons.

MATERIALS AND METHODS

Five adult cats, including two control animals, were used. Anaesthesia was induced by intraperitoneal injection of sodium pentobarbitone (45 mg/kg).

Injection of horseradish peroxidase

In three anaesthetised cats, an incision was made between the sixth and thirteenth dorsal thoracic vertebral spinous processes after shaving and cleansing the skin. Lateral retraction of the skin and underlying latissimus dorsi muscle exposed a portion of the erector spinae. In the ninth or tenth intercostal space, both the levator costae and external intercostal muscles were exposed unilaterally by retracting longissimus thoracis medially and removing a portion of iliocostalis thoracis between its costal attachments.

To limit diffusion of horseradish peroxidase (Sigma, type VI), the levator costae and proximal 15 mm of the external intercostal muscles were coated with a film of 5 % Agar in distilled water at a temperature of between 40–50 °C on application, but which cooled and set almost immediately on tissue contact. A glass microelectrode,

tip diameter 100 μm, was filled with 10–20 μl of 40% horseradish peroxidase in saline and 2–5 μl aliquots injected through the Agar into one or both muscles at several sites using a micrometer syringe.

The wound was closed with sutures and the animals allowed to survive for 24 hours.

Perfusion and histochemistry

One control and all experimental animals were anaesthetised and perfused via the abdominal aorta with a fixative mixture consisting of 2% glutaraldehyde and 1% paraformaldehyde in 0·1 M sodium phosphate, pH 7·4, at 20 °C, after briefly flushing the vascular system with saline. The remaining control animal from which tissue was made available formed part of a study by Pullen & Sears (1978) and had been perfused instead with 2·5% glutaraldehyde and 2% paraformaldehyde in 0·2 M sodium cacodylate, pH 7·4.

In experimental animals, transverse slices 70 μm thick of fixed spinal cord at T9 or T10 were cut using a Vibroslice vibrating blade tissue slicer (Jefferys, 1982) and processed to demonstrate peroxidase activity (Adams, 1977). Slices treated with osmium tetroxide were subsequently dehydrated in an ascending series of ethanol solutions, equilibrated with Araldite via an intermediate stage in propylene oxide and flat-embedded in a thin layer of Araldite between two polytetrafluoroethylene-coated microscope slides (Romanovicz & Hanker, 1977)

In control animals, 1–2 mm slices of aldehyde-fixed spinal cord from T9 were routinely postfixed in osmium tetroxide, dehydrated and embedded in Araldite.

Light microscopy

Using bright field illumination, the cell bodies of retrogradely labelled motoneurons were identified within 70 μm Araldite-embedded slices by the presence of black granules of reaction product in their cytoplasm. To estimate the size range of labelled motoneurons, their cell body diameters were determined with the aid of an ocular graticule. Measurements were made with nucleoli in the plane of focus by enclosing an imaginary ellipse within the confines of the cell body and recording the maximum and minimum diameters.

Electron microscopy

The portion of the ventral horn containing labelled motoneurons was excised and glued to a polished Araldite cylinder. Transillumination of this cylinder enabled the labelled motoneurons to be seen and guided trimming of the specimen so that such motoneurons could be located in relation to both the sides of the 'mesa' and internal landmarks, such as blood vessels. The same motoneurons were re-identified in 0·5 μm thick sections stained with toluidine blue and subsequently in adjacent ultrathin (60–100 nm) sections stained with uranyl acetate and lead citrate and examined in a Philips 301, a Jeol 100c or a Jeol 120cx electron microscope.

Quantitative methods

Twenty small labelled motoneurons, together with 10 large labelled motoneurons and 10 large normal, unlabelled, motoneurons, were measured on electron micrograph photomontages at final magnifications of $\times$10000 (large motoneurons) or $\times$19000 (small motoneurons). These different magnifications standardised the final

size of the cell body montages and so facilitated their accommodation on the plotting tablet, but did not affect the accuracy of any measurements made.

Areas and lengths were measured with the aid of a digitised plotting tablet connected to a mini-computer. All measurements were restricted to the cell body and where necessary, a smooth contoured line was drawn across the base of dendrites between the points of greatest inflection of somatic and dendritic membrane to delineate cell body boundaries. No corrections for tissue shrinkage were made, neither were derived parameters adjusted for the effects of particle shape, number or distribution in relation to section thickness.

Synaptic terminals

All synaptic terminals apposing the plasma membrane were quantified, irrespective of whether pre- and postsynaptic densities were present. The number of terminals per 100 μm length of plasma membrane was recorded as 'synaptic frequency' and their lengths of apposition per 100 μm plasma membrane recorded as 'synaptic cover'.

Nuclear pores

The point where inner and outer nuclear membranes apposed to form a thin diaphragm, delineated on both nuclear and cytoplasmic aspects by an electron-dense filamentous corona, constituted a nuclear pore. Since nuclear pores were only 70 nm in diameter, the presence of densities alone was taken as a good approximation of their position. The number of nuclear pores per 100 μm nuclear membrane was recorded as the 'nuclear pore frequency'.

Lysosomes

All electron-dense, membrane-delineated bodies were classed as lysosomes, even though some may not have contained acid phosphatase (De Duve, 1963; Novikoff, 1967). Attempts to differentiate between primary and secondary lysosomes were abandoned due to the variability introduced by such factors as section thickness, degree of staining and intensity of retrograde labelling. The number of lysosomes per 100 μm^2 cytoplasm was recorded as 'lysosomal frequency'.

Golgi apparatus

The cisternae and vesicles of individual Golgi profiles were encompassed within a single boundary line, with no attempt to segregate the histochemically defined GERL complex (Novikoff & Novikoff, 1977). The numbers or areas of these units/ 100 μm^2 cytoplasm were recorded as 'Golgi frequency' or 'Golgi area' respectively.

Nissl bodies

Nissl bodies associated with C-type synapses have been defined (Pullen & Sears, 1983) as aggregates of parallel cisternae of granular endoplasmic reticulum, with linear arrays of polyribosomes interposed between adjacent cisternae and surrounded by a variable number of randomly sited polyribosomes. The generality of this description for Nissl bodies elsewhere in the motoneuronal cytoplasm has been established through closely correlated light and electron microscopy of individual Nissl bodies (Johnson, 1983). However, such heterogeneous structures, characterised more by their internal orderliness than by their constituent elements, did not lend themselves to conventional stereological analyses. Therefore a Nissl body was

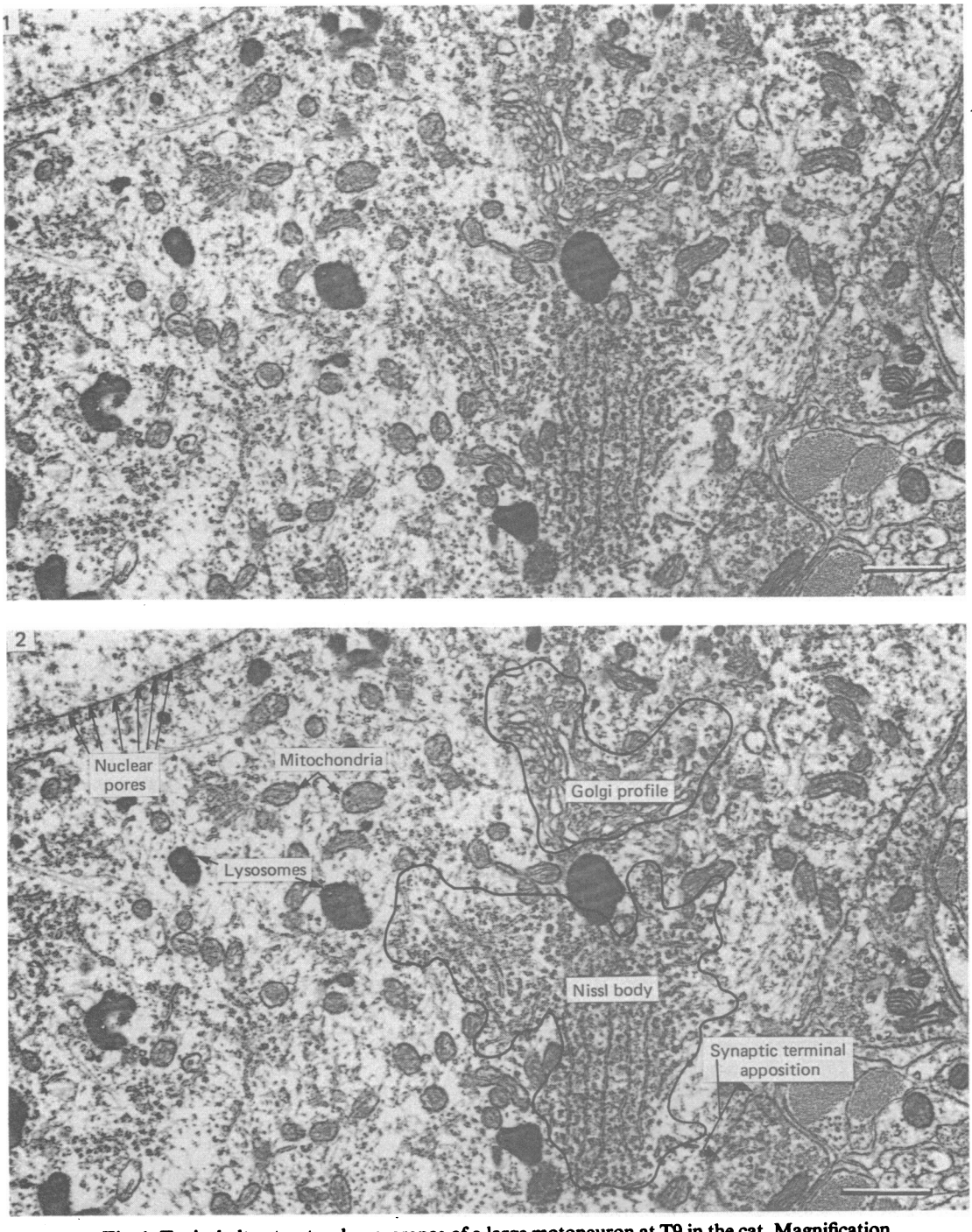

Fig. 1. Typical ultrastructural appearance of a large motoneuron at T9 in the cat. Magnification as in Figure 2.

Fig. 2. The same motoneuron shown in Figure 1. illustrating the definitions of organelles and their boundaries as employed for quantitative analyses. Bar, 1·0μm.

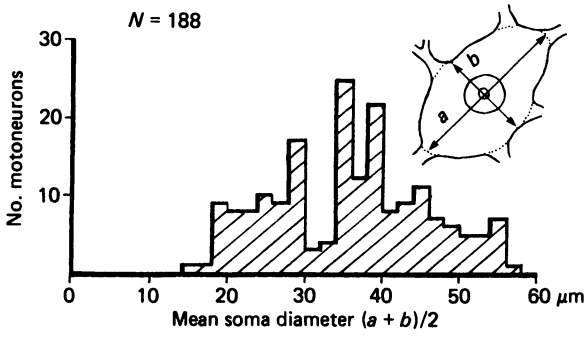

Fig. 3. Frequency histogram (2 μm interval) of mean cell body diameters of 188 retrogradely labelled cat thoracic motoneurons, illustrating the wide range of neuronal sizes present.

defined operationally as 'an aggregate of three or more parallel cisternae of granular endoplasmic reticulum, together with any associated polyribosomes'. The boundaries of such a Nissl body were taken as the points where a marked reduction in polyribosomal packing density occurred. These boundaries were marked on the montages and the numbers or areas of Nissl bodies per 100 μm^2 cytoplasm recorded as 'Nissl frequency' or 'Nissl area' respectively.

Figures 1 and 2 illustrate the definitions of organelles and their boundaries as employed in this study.

Student's *t*-test was used to assess the significance of differences between sample means.

RESULTS

Light microscopy

Location and size of motoneurons

Both large and small motoneurons were intermingled, with levator costae motoneurons located in the ventromedial tip of the ipsilateral ventral horn and external intercostal motoneurons located more dorsolaterally. This confirms previous reports on the locations of these particular motoneurons (Coffey, 1972; Fedorko, 1982).

The mean diameters (Fig. 3) recorded for 188 labelled motoneurons within slices 70 μm thick ranged from 14 to 56 μm, with a sample mean of 35 μm. On the basis of the shape of a frequency histogram of cell diameters (Fig. 3), a 'large motoneuron' was taken as one where the mean cell body diameter was greater than 40 μm and a 'small motoneuron' as one where the mean cell body diameter was less than 30 μm. Those motoneurons with mean diameters between 30–40 μm were ignored in subsequent morphological analyses in order to make this distinction between large and small motoneurons more clearcut. Large and small motoneurons were selected randomly, with no attempt to segregate levator costae or external intercostal motoneurons.

Structure of motoneurons

Through-focus analyses of labelled motoneurons in slices 70 μm thick post-fixed with osmium tetroxide revealed several stout proximal dendrites radiating from large motoneurons, whereas proximal dendrites radiating from small motoneurons were thinner and fewer in number (Fig. 4). In sections stained with toluidine blue (Fig. 5), both large and small motoneurons had a similar intracellular appearance, displaying coarse Nissl bodies, a pale, centrally located nucleus and a prominent nucleolus.

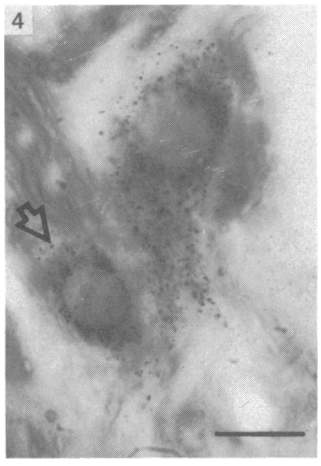

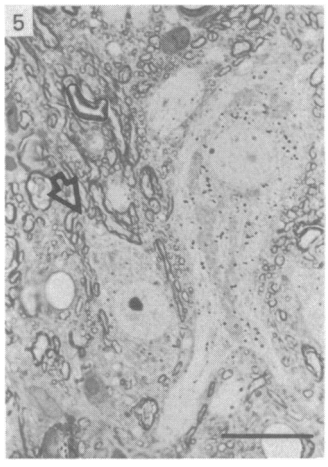

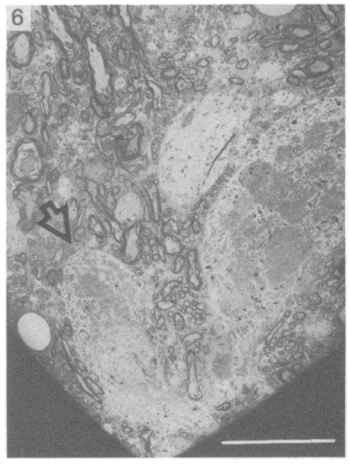

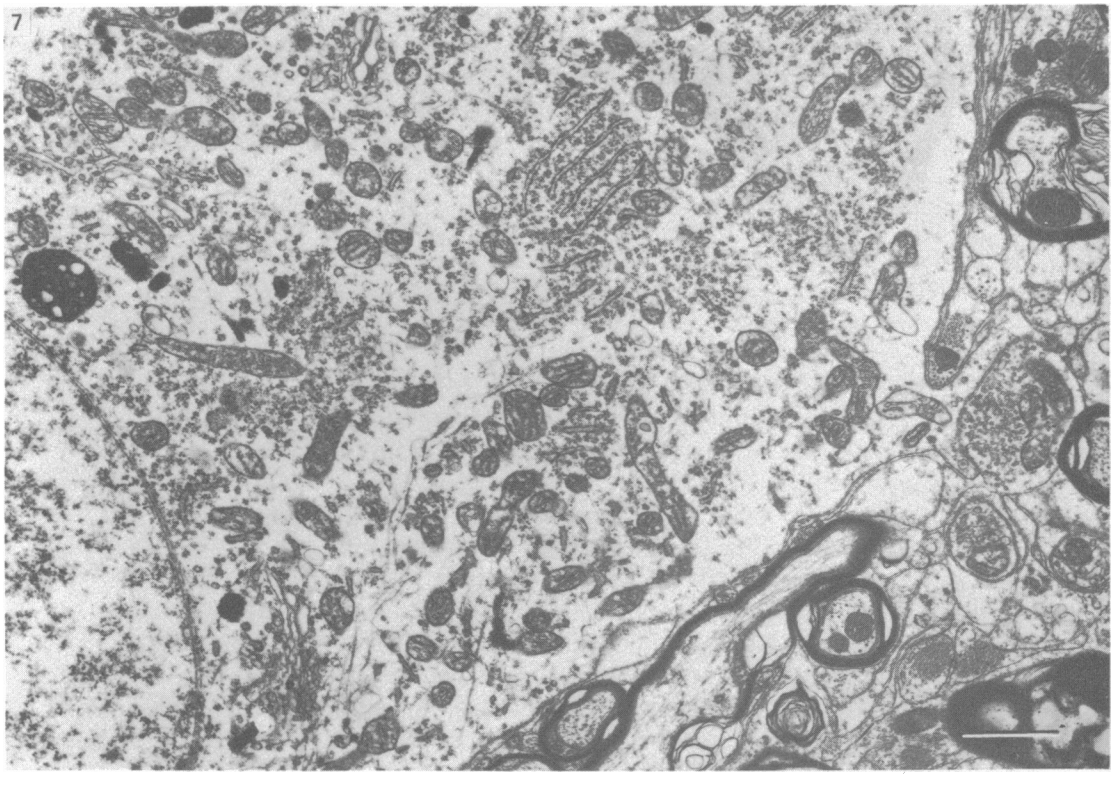

Fig. 4. Small retrogradely labelled motoneuron (arrow) adjacent to a large motoneuron at T10, 24 hours following horseradish peroxidase injection into the ipsilateral levator costae muscle. Two stout dendrites radiate from the large motoneuron. 70 μm section postfixed in osmium tetroxide and embedded in Araldite. Bar, 25 μm.

Fig. 5. The same motoneurons shown in Figure 4. 0·5 μm toluidine blue-stained section showing the similar appearance of both cell bodies. Bar, 25 μm.

Fig. 6. Survey electron micrograph of the same motoneurons shown in Figures 4 and 5, demonstrating the correlative approach employed to identify labelled motoneurons by electron microscopy. Bar, 25 μm.

Fig. 7. General ultrastructural organisation of the small motoneuron arrowed in Figures 4, 5 and 6, illustrating a similarity to the ultrastructure of the large motoneuron shown in Figure 1. Bar, 1·0 μm.

Electron microscopy

Qualitative observations

A comparison of (i) large normal motoneurons, (ii) large labelled motoneurons, and (iii) large unlabelled (but histochemically processed) motoneurons revealed that the histochemical procedure produced mild splitting of myelin lamellae with some mitochondrial vacuolation. Dense bodies appeared to be more conspicuous in labelled motoneurons but in all other respects, labelling and histochemical processing had no obvious effect on motoneuronal ultrastructure. Furthermore, the use of a fixative of different concentrations in one normal animal had no qualitative or quantitative effect on motoneuronal ultrastructure, although the more hypertonic fixative did result in better preservation of white matter.

Intracellular features

While the general ultrastructural organisation of both large and small motoneuronal cytoplasm was similar (compare Figs. 1 and 7), neurofilaments and neurotubules were less conspicuous in small motoneurons, rendering their cytoplasm more electron-lucent (Fig. 10).

Synaptic terminals

Marked differences between large and small motoneurons were evident when the synaptic terminals apposing their cell bodies were compared. In both relative and absolute terms, considerably more synaptic terminals were seen on large as opposed to small motoneurons. Where proximal dendrites were seen to extend from labelled motoneuronal cell bodies, it was evident that for both large and small motoneurons the number of synaptic terminals per unit length of dendritic membrane was approximately twice that seen on the cell body.

A more detailed analysis of synaptic terminals on large motoneurons revealed that four of the six synaptic types described by Conradi (1969) on cat lumbar motoneurons were consistently present. These were the S-type (round synaptic vesicles and asymmetrical synaptic densities), the F-type (flattened synaptic vesicles and symmetrical synaptic densities), the T-type (as for S-type, but with postsynaptic dense 'Taxi' bodies) and the C-type (round synaptic vesicles, a subsynaptic, agranular cistern and a postsynaptic Nissl body). The M-type synapse, with its associated P-terminal was seen only once. These synaptic types have previously been reported on large intercostal motoneurons in the cat by Pullen & Sears (1983).

When a similar analysis of the synaptic types present on small motoneurons was made, only S- and F-type synapses were observed (Figs. 11, 12). In particular, the large, distinctive C-type synapse (Fig. 13) was not seen on any small motoneuron.

Quantitative observations

Values for various aspects of large and small motoneuronal ultrastructure are summarised in Table 1. The only features for which statistically significant differences between samples were found were Nissl body size, synaptic features and lysosomal frequency.

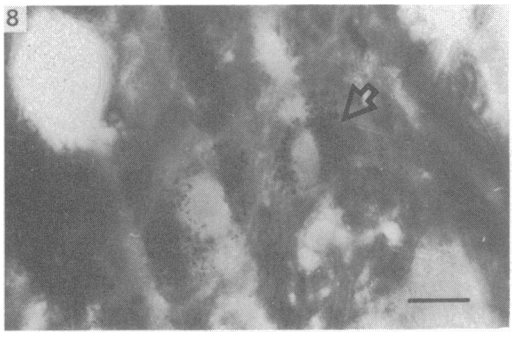

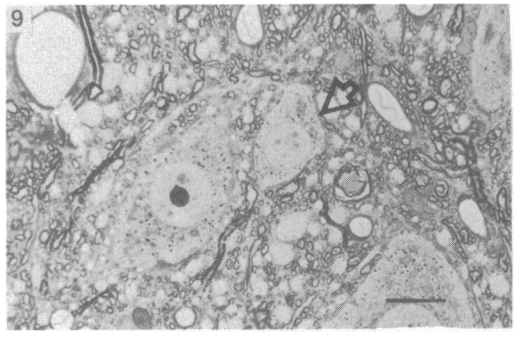

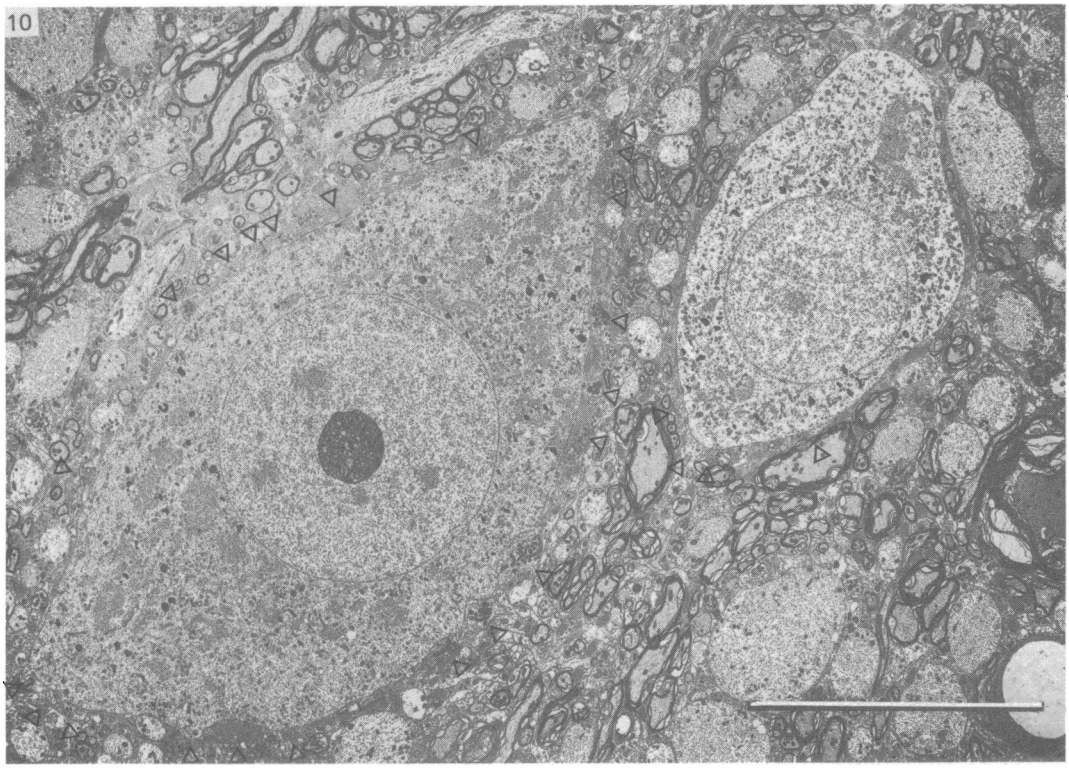

Fig. 8. Small retrogradely labelled motoneuron (arrowed) adjacent to a large motoneuron at T10, 24 hours following horseradish peroxidase injection into the ipsilateral levator costae and external intercostal muscles. 70 μm section postfixed in osmium tetroxide and embedded in Araldite. Magnification as in Figure 9.

Fig. 9. Same motoneurons as shown in Figure 8. 0·5 μm toluidine blue-stained section. Bar, 25 μm.

Fig. 10. Electron micrograph of the same motoneurons shown in Figures 8 and 9. Far fewer synaptic terminals (indicated by arrowheads) are seen over the small motoneuron than over the large motoneuron. Bar, 25 μm.

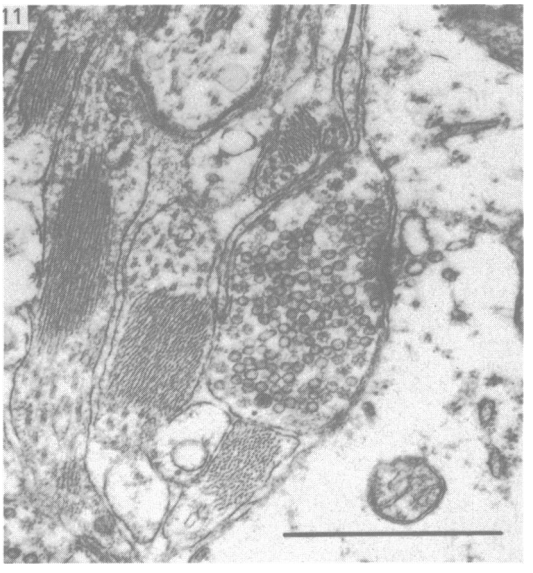

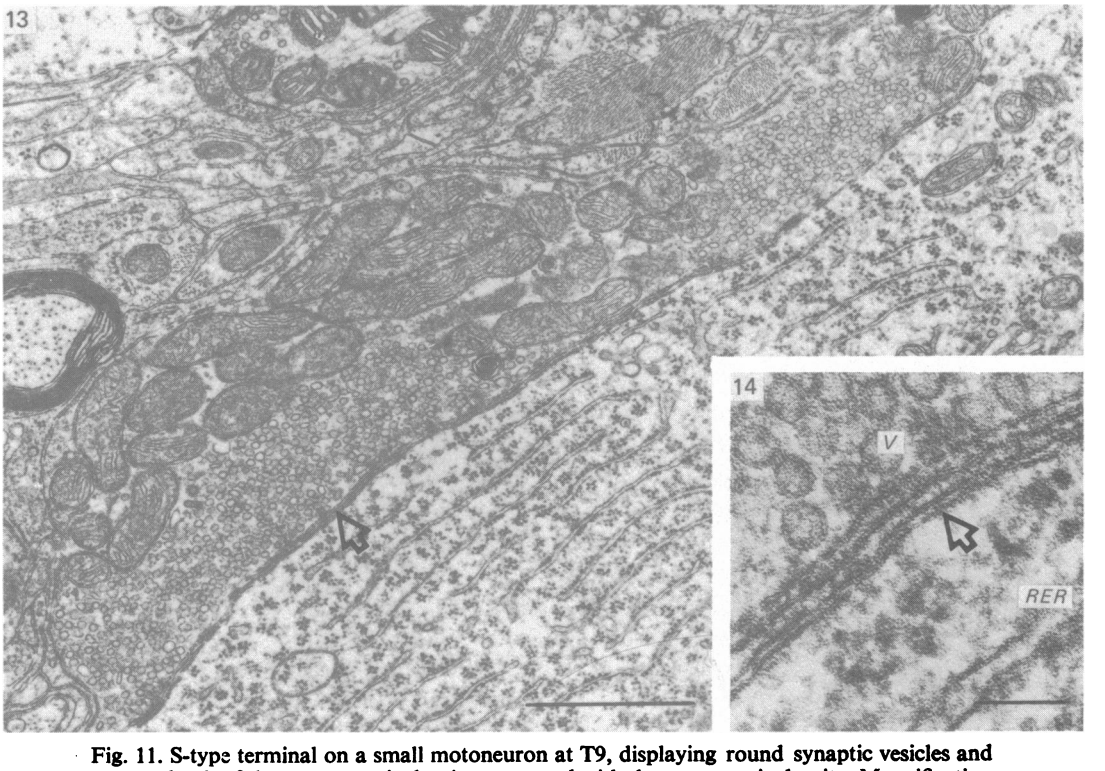

Fig. 11. S-type terminal on a small motoneuron at T9, displaying round synaptic vesicles and greater depth of the postsynaptic density compared with the presynaptic density. Magnification as in Figure 12.

Fig. 12. F-type synaptic terminal on a small motoneuron at T9, displaying elongated vesicles and pre- and postsynaptic densities of similar depths. Bar, 1·0 μm.

Fig. 13. C-type synaptic terminal on a large motoneuron at T9, displaying round synaptic vesicles within a large presynaptic terminal, absence of pre- and postsynaptic densities, an agranular subsynaptic cistern (arrowed) and a postsynaptic stack of organised granular endoplasmic reticulum. Bar, 1·0 μm.

Fig. 14. Detail of a C-type synapse showing vesicles (*V*), the subsynaptic cistern (arrowed) and a portion of granular endoplasmic reticulum (*RER*). Bar, 0·1 μm.

Table 1. *Quantitative aspects of large and small motor neuron ultrastructure*

Feature	(A) Large normal	(B) Large labelled	(C) Small labelled	t-Tests A vs B	A vs C	B vs C
Nissl frequency	1·54±0·79	1·85±0·78	0·79±0·44	N.S.	**	***
Nissl area	8·84±4·58	7·66±3·06	6·91±5·54	N.S.	N.S.	N.S.
Mitochondrial frequency	88·31±28·53	98·95±21·79	92·42±22·12	N.S.	N.S.	N.S.
Lysomal frequency	15·10±3·56	23·80±7·45	23·57±9·39	**	**	N.S.
Nuclear pore frequency	322·6±66·04	322·5±87·5	345·1±95·7	N.S.	N.S.	N.S.
Golgi frequency	2·34±0·69	2·62±0·69	2·72±0·87	N.S.	N.S.	N.S.
Golgi area	3·28±0·76	4·46±1·85	5·22±2·57	N.S.	N.S.	N.S.
Total synaptic cover	34·35±13·16	34·65±10·66	16·60±12·98	N.S.	**	***
Synaptic cover (round vesicles)	15·34±4·74	16·71±7·33	6·71±5·88	N.S.	***	***
Synaptic cover (flat vesicles)	18·99±9·22	17·94±8·28	9·89±9·64	N.S.	*	*
Total synaptic frequency	18·49±8·70	16·16±4·85	9·00±7·28	N.S.	**	**
Synaptic frequency (round vesicles)	7·93±3·76	7·28±2·10	3·68±3·16	N.S.	**	**
Synaptic frequency (flat vesicles)	10·56±5·26	8·88±3·63	5·33±5·44	N.S.	*	*

$x \pm$ S.D.; N.S., $P > 0{\cdot}05$; *, $P < 0{\cdot}05$; **, $P < 0{\cdot}01$; ***, $P < 0{\cdot}001$.

Lysosomes

Large labelled motoneurons had over 50 % more lysosomes than did large normal motoneurons. In contrast, both large labelled motoneurons and small labelled motoneurons had similar values for lysosomal frequency.

Nissl bodies

While Nissl area was similar for both large and small motoneurons, Nissl frequency was lower in the small cells. This was largely due to the presence of more smaller sized Nissl bodies in large motoneurons.

Synaptic terminals

Synaptic cover and frequency on small motoneurons was less than half that on large motoneurons. When this synaptic difference was analysed in terms of synaptic terminals with round (S- T- and C-types) or flattened (F-type) synaptic vesicles, both synaptic groups had lower values on small motoneurons, the magnitude of the reduction being greatest for synaptic terminals with round vesicles.

In confirmation of a previous report on a smaller sample (Johnson, 1985), considerable variability of synaptic terminal frequency and cover between individual small motoneurons was found. In the present study, for a total of 160 synaptic terminals spread over 1640 μm plasma membrane and 20 small motoneurons, values for synaptic cover and frequency showed standard deviations up to 80 % of the respective mean values. In contrast, for similar total synaptic terminal numbers or total plasma membrane length, the corresponding standard deviations for the same parameters on large motoneurons amounted to only 30–40 % of their respective mean values. Thus, small motoneurons exhibited twice the synaptic variability of large motoneurons.

Correlations with cell size

When values for all the features listed in Table 1 for small motoneurons were compared with mean cell body diameter, no correlation was indicated, either by

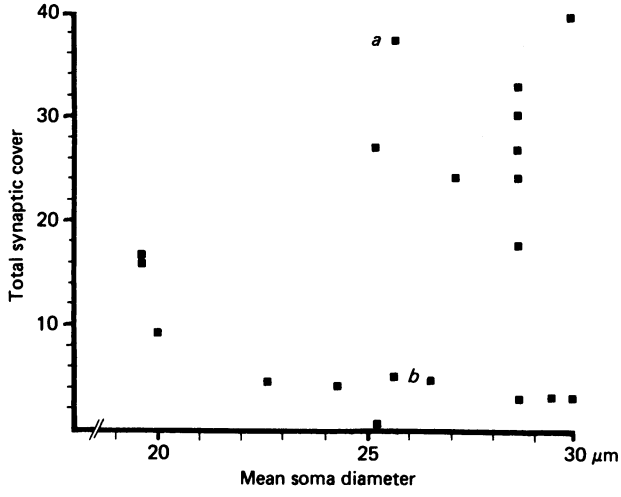

Fig. 15. Graph of total synaptic terminal cover on 20 small motoneurons against mean soma (cell body) diameter. Two groupings of cells are seen, one, with values > 20, the other with values < 20. Two cell bodies, a and b, from these groups are illustrated in Figures 16 and 17.

scatter diagrams or calculation of the linear regression coefficient. Nevertheless, the impression was gained that small motoneurons fell into two categories: one with synaptic terminal values in the large motoneuron range and one with low synaptic terminal values. This impression was borne out visually in scatter diagrams for all aspects of synaptic cover (Fig. 15), but not for synaptic frequency. A comparison of similarly sized small motoneurons with either 'high' or 'low' values for synaptic cover (Fig. 15*a*, *b*), failed to reveal any obvious intracellular feature which might suggest the presence of two subpopulations of small motoneurons (Figs. 16, 17).

DISCUSSION

In the present investigation, a qualitative and quantitative ultrastructural comparison of large and small motoneurons in the thoracic spinal cord was undertaken using horseradish peroxidase as a retrograde neuronal marker to distinguish motoneurons from interneurons. Large and small motoneurons had similar intracellular appearances but exhibited marked differences in the features of their respective synapses, which may have implications for the suggested functional roles of these two motoneuronal types.

Motoneurons and interneurons

Retrograde trans-synaptic labelling of spinal interneurons in rats and cats has been reported using wheat germ agglutinin conjugated to horseradish peroxidase (Harrison *et al.* 1984). Using a highly sensitive chromagen (tetramethylbenzidine), the above authors reported that lightly labelled interneurons are located well away from the more heavily labelled pools of motoneurons in the ipsilateral ventral horn. Similarly, Coffey (1972) has found that cat thoracic interneurons, identified on the basis of their chromatolytic response to near hemisection of the spinal cord, are largely located outside the motoneuron pools of the ventral horn. In relation to the present study, the retrograde trans-synaptic labelling of mammalian spinal interneurons has not been demonstrated using horseradish peroxidase alone. Moreover,

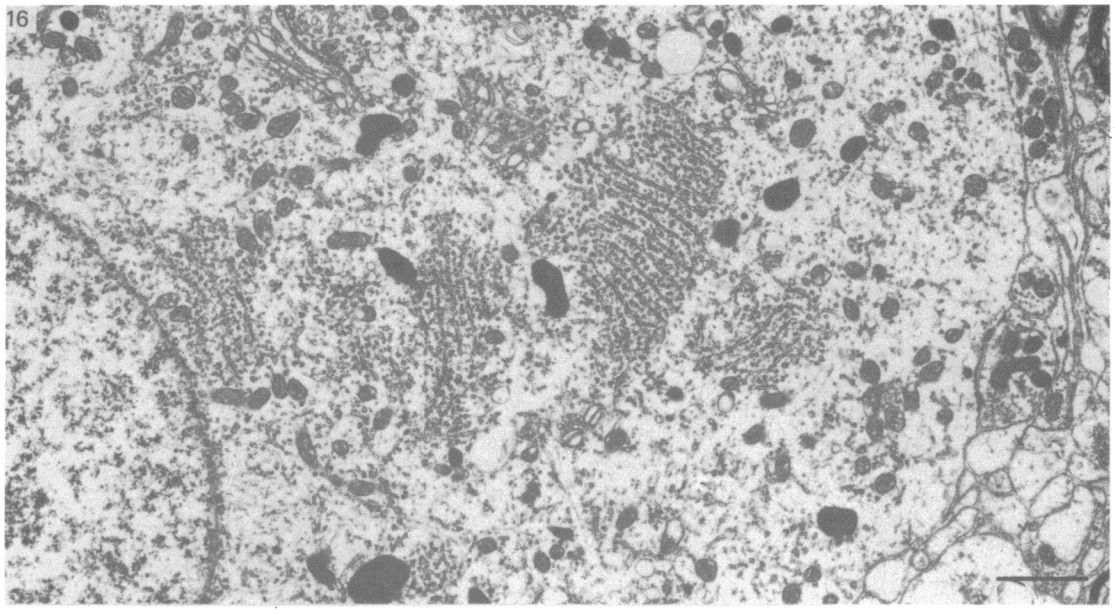

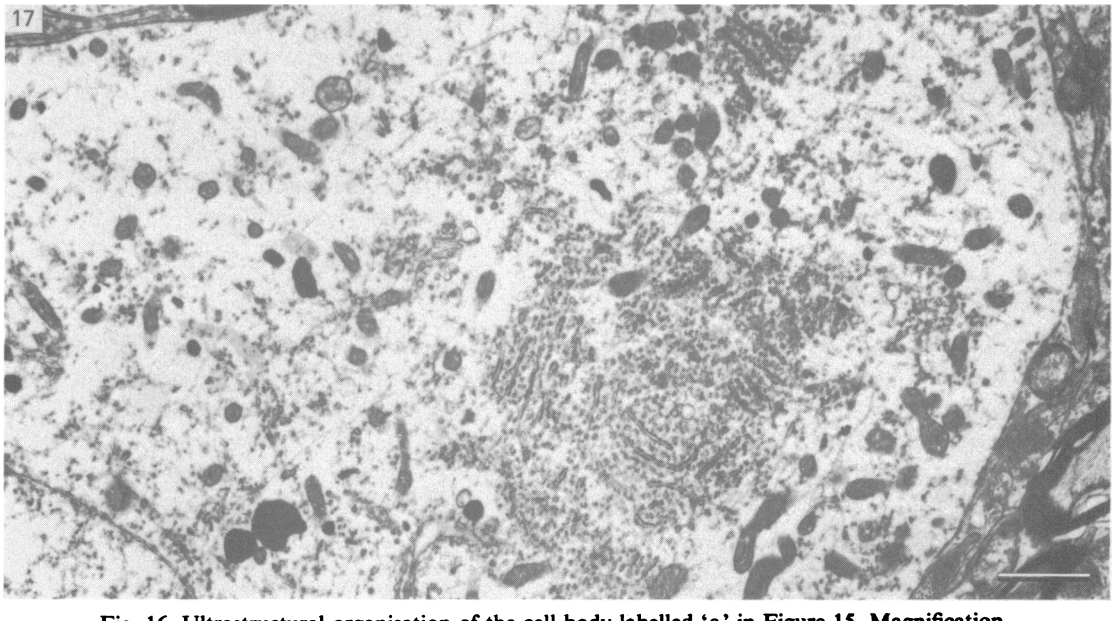

Fig. 16. Ultrastructural organisation of the cell body labelled 'a' in Figure 15. Magnification as in Figure 17.

Fig. 17. Ultrastructural organisation of the cell body labelled 'b' in Figure 15. While Nissl bodies appear less well organised than in Figure 16, this is a variable feature and, overall, no specific intracellular feature distinguishes motoneurons with relatively high or low synaptic terminal coverage. Bar, 1·0 μm.

where a less sensitive chromagen (diaminobenzidine) has been used, labelled cell bodies in the thoracic spinal cord are not observed outside the ipsilateral ventral horn motor pools. The possibility of interneuronal contamination of the present motoneuronal sample is therefore considered to be remote.

Alpha and gamma motoneurons

In the cat, a bimodal distribution of motor axon diameters has been found in the nerves to the gastrocnemius, soleus and the external intercostal muscles (Eccles & Sherrington, 1930; Sears, 1964*a*). A similar distribution of cat gastrocnemius/soleus motor neuron cell bodies has also been reported (Burke *et al.* 1977) and, in the present study, a bimodal distribution of external intercostal plus levator costae motoneuronal cell body diameters has been found (Fig. 3). For both the cat hindlimb and thoracic musculature, large diameter, fast conducting 'alpha' motor axons supply extrafusal muscle fibres which are responsible for generating changes in external muscle tension, whereas small diameter, slowly conducting 'gamma' motor axons innervate intrafusal muscle fibres of the muscle spindle and are responsible for regulating its sensitivity to stretch (Leksell, 1945; Kuffler, Hunt & Quilliam, 1951; Andersen & Sears, 1964). Since large diameter cell bodies usually give rise to large diameter axons and *vice versa*, large and small motoneuronal cell bodies have classically been equated with alpha and gamma motoneurons respectively. The validity of this assumption has been borne out for electrophysiologically identified alpha and gamma motoneurons in the cat lumbosacral spinal cord where the respective range of cell body diameters is reported as 40·0–75·5 μm and 25·5–39·5 μm (Westbury, 1979; Brown & Fyffe, 1981; Ulfhake & Cullheim, 1981). Since this range of cell body diameters is similar to the large (> 40 μm) and small (< 30 μm) motoneurons examined in the present study, it is suggested that the large and small motoneurons constitute alpha and gamma motoneurons respectively, although electrophysiological verification is still required to substantiate this view fully.

While motoneurons innervating both intra- and extrafusal muscle (beta motoneurons) have been identified electrophysiologically in several muscles of the cat hindlimb (Emonet-Dénand & Laporte, 1975), neither their morphology nor the extent of their occurrence in thoracic nerves of the cat is known. Whether beta motoneurons were included in the present sample of motoneurons is therefore uncertain.

Intracellular features

The assumption that neither the retrograde axonal transport of horseradish peroxidase nor the subsequent histochemical processing altered motoneuronal structure was largely borne out by control observations. However, the detection of a 50% increase in lysosomal frequency over normal contrasts with both the absence of any qualitative increase in acid phosphatase levels in retrogradely labelled mouse hypoglossal motoneurons (Broadwell & Brightman, 1979) and the absence of any qualitative change in lysosomal frequency or structure, when this aspect was specifically examined in retrogradely labelled neurons of the inferior olive in cats (Osculati *et al.* 1980). In the absence of additional enzyme histochemical data, it is not possible to state whether the present lysosomal increase was real or simply because the electron density of the reaction product within cytoplasmic vesicles made them more visible in electron micrographs. Whatever the mechanism of the lysosomal

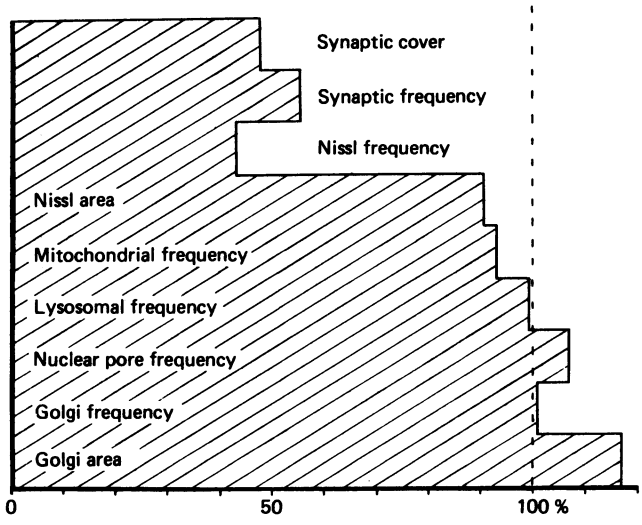

Fig. 18. Values for various aspects of gamma motoneuronal ultrastructure expressed as percentages of labelled alpha motoneuron values. Gamma motoneurons differ in terms of synaptic cover, synaptic frequency and Nissl frequency.

increase, it affected retrogradely labelled alpha and gamma motoneurons equally (Fig. 18) and is not considered to be a distinguishing feature.

Both alpha and gamma motoneurons had a very similar intracellular appearance. This might reflect a basic metabolic similarity, perhaps related to their common function as final cellular links between the spinal cord and muscle. However, in a light microscopic histochemical study by Campa & Engel (1970) of large and small motoneurons in the lumbar ventral horn of cats, neurons with diameters below 30 μm had high levels of succinate dehydrogenase staining and very low levels of phosphorylase staining, while the reverse was true for neurons larger than 30 μm in diameter. Although these findings might reasonably be adduced to the present result on the structure of alpha motoneurons, this cannot be done in the case of gamma motoneurons, since Campa & Engel did not distinguish small motoneurons from interneurons with their method of analysis. Indeed, it has been estimated that interneurons outnumber motoneurons by three to one within the peroneus-tibialis motor pool in the cat (Balthazar, 1952).

Synaptic features

Apart from size, the single most distinguishing feature of gamma motoneurons was their paucity of synapses, leaving large stretches of cell body membrane covered by astroglial processes and the occasional oligodendrocyte. Even when synaptic frequency and cover approximately doubled on gamma motoneuronal proximal dendrites, it was still considerably lower than the corresponding synaptic frequency or cover on alpha motoneuronal proximal dendrites. Gamma motoneurons labelled by intracellular injection of horseradish peroxidase after electrophysiological identification have only about half the number of proximal dendrites of similarly labelled alpha motoneurons; furthermore, the dendrites of gamma motoneurons are thinner and branch less frequently (Westbury, 1982; Ulfhake & Cullheim, 1981). These differences in cellular geometry, together with the present observations on synaptic terminals suggest that gamma motoneurons neither receive nor are capable of

receiving anywhere near the number of synaptic terminals that impinge on alpha motoneurons.

On the basis that the small motoneurons examined here are gamma motoneurons, three features of their synaptic organisation have potential functional significance. Firstly, the considerable between-cell variation observed for gamma motoneuronal synapses may reflect the very wide range of discharge frequencies found for cat thoracic gamma motoneurons (Sears, 1964*b*) and also the marked variation found between individual cat lumbosacral gamma motoneurons in response to stimulation of various afferent nerves (Appelberg, Hulliger, Johansson & Sojka, 1983). Secondly, the apparent segregation of gamma motoneurons into two groups, one with very low synaptic cover and the other with synaptic cover approximating to that of alpha motoneurons (Fig. 15), may reflect the existence of two physiologically distinct gamma motoneuronal populations in the form of gamma-dynamic and gamma-static motoneurons, both of which have different afferent inputs and firing patterns (Matthews, 1972; Appelberg, 1981). Thirdly, if it is accepted that motoneuronal excitability is inversely related to cell size (Henneman, Somjen & Carpenter, 1965; Henneman & Mendell, 1981), the failure in the present study to correlate gamma motoneuronal synaptic frequency or cover with cell body diameter calls in question the importance of synaptic terminal density (Burke, 1981), at least on the cell body, as a major factor governing motoneuronal excitability. These comments must, however, be regarded as tentative since much basic information on the electrical properties of gamma motoneuronal membranes, the nature and efficiency of their synapses and the synaptic organisation of their dendrites is as yet unknown.

In a total of 20 alpha motoneurons quantified, 16 out of 405 synaptic terminals (4·0 %) were C-type synapses. By contrast, no C-type synapses were seen out of 160 synaptic terminals quantified on 20 gamma motoneurons. Together with the fact that C-type synapses were not seen on any small neurons in the cat thoracic spinal cord, it must be assumed that C-type synapses are absent on gamma motoneurons. Since only 2 T-type (0·5 %) and no M-type synapses were found on the 20 alpha motoneurons quantified, the failure to find T- and M-type synapses on any gamma motoneuron, including those not quantified, can only be taken as a tentative indication of their absence.

Believed to be primarily of local interneuronal origin, C-type synapses increase in both size and number on partially deafferented thoracic motoneurons (Pullen & Sears, 1978). The postsynaptic Nissl body associated with the C-type synapse also hypertrophies under these conditions and this has led to the view that the C-type synapse mediates a trophic interaction between motoneurons and interneurons. In, general motoneuronal synapses are particularly sensitive to perturbations of contact of the motoneuron with its peripheral target, as shown by the synaptic loss following axotomy or blockade of axonal transport (Blinzinger & Kreutzberg, 1968; Cull, 1975; Chen, 1978). The general paucity of synapses on gamma as opposed to alpha motoneurons, may reflect a different mode of interaction with targets in the periphery. Experiments comparing the synaptic response of alpha and gamma motoneurons to axotomy are currently in progress to investigate the nature of this interaction.

SUMMARY

The cell bodies of motoneurons supplying both the levator costae and external intercostal muscles were identified after retrograde labelling with horseradish peroxidase. A quantitative ultrastructural comparison of cell bodies of large ($> 40\ \mu m$) and small ($< 30\ \mu m$) diameter revealed that the intracellular appearance of large and small motoneurons was similar. However, small motoneurons had less than half the synaptic terminal frequency or cover of large motoneurons. Furthermore, only synapses of the S- and F-type were seen on small motoneurons, while S- T- F- and C-type terminals were consistently seen on large motoneurons. The variation between individual small motoneurons for various aspects of their synaptic features was more than twice that found for large motoneurons.

No correlation between small motoneuronal ultrastructure and cell body diameter was found, although scatter diagrams of synaptic terminal cover against cell body size indicated the presence of two groups of small motoneurons: one with relatively high values for synaptic cover and the other with relatively low values.

On the basis of the similarity of their cell body diameters to those of electrophysiologically identified alpha and gamma motoneurons, it is concluded that the large and small motoneurons examined in the present study are alpha and gamma motoneurons respectively. The synaptic difference found between alpha and gamma motoneurons is discussed in relation to both their different functional properties and the different natures of their respective peripheral targets.

The author thanks Professor T. A. Sears and Dr A. H. Pullen for their advice and encouragement. The study was supported by a grant to Professor Sears from the Multiple Sclerosis Society.

REFERENCES

ADAMS, J. C. (1977). Technical considerations on the use of horseradish peroxidase as a neuronal marker. *Neuroscience* **2**, 141–145.

ANDERSEN, P. & SEARS, T. A. (1964). The mechanical properties and innervation of fast and slow motor units in the intercostal muscles of the cat. *Journal of Physiology* **173**, 114–129.

APPELBERG, B. (1981). Selective control of dynamic gamma motoneurones utilized for the functional classification of gamma cells. In *Muscle Receptors and Movement* (ed. A. Taylor & A. Prochazka), pp. 97–108. London: Macmillan.

APPELBERG, B., HULLIGER, M., JOHANSSON, H. & SOJKA, P. (1983). Actions on γ-motoneurones elicited by electrical stimulation of group III muscle afferent fibres in the hind limb of the cat. *Journal of Physiology* **335**, 275–292.

BALTHAZAR, K. (1952). Morphologie der spinalen Tibialis – und Peronaeus-Kerne bei der Katze. *Archiv für Psychiatrie und Nervenkrankheiten* **188**, 342–378.

BLINZINGER, K. & KREUTZBERG, G. (1968). Displacement of synaptic terminals from regenerating motoneurones by microglial cells. *Zeitschrift für Zellforschung und mikroskopische Anatomie* **85**, 145–157.

BROADWELL, R. D. & BRIGHTMAN, M. W. (1979). Cytochemistry of undamaged neurons transporting exogenous protein *in vitro*. *Journal of Comparative Neurology* **185**, 31–74.

BROWN, A. G. & FYFFE, R. E. W. (1981). Direct observations on the contacts made between afferent fibres and α-motoneurones in the cat's lumbosacral spinal cord. *Journal of Physiology* **313**, 121–140.

BRYAN, R. N., TREVINO, D. L. & WILLIS, W. D. (1972). Evidence for a common location of alpha and gamma motoneurones. *Brain Research* **38**, 193–196.

BURKE, R. E. (1981). Motor units: anatomy, physiology and, functional morphology. In *Handbook of Physiology*, sect. 1, vol. II, part 1 (ed. J. M. Brookhart & V. B. Mountcastle), pp. 345–422. Bethesda, Maryland: American Physiological Society.

BURKE, E. E., STRICK, P. L., KANDA, K., KIM, C. C. & WALMSLEY, B. (1977). Anatomy of medial gastrocnemius and soleus motor nuclei in cat spinal cord. *Journal of Neurophysiology* **40**, 667–680.

CAMPA, J. F. & ENGEL, W. K. (1970). Histochemistry of motor neurons and interneurones in the cat lumbar spinal cord. *Neurology* **20**, 559–569.

CHEN, D. H. (1978). Qualitative and quantitative study of synaptic displacement in chromatolysed spinal motoneurones of the cat. *Journal of Comparative Neurology* **177**, 635–664.

COFFEY, G. L. (1972). The distribution of respiratory motoneurones in the thoracic spinal cord of the cat. Ph.D. thesis, University of London.

CONRADI, S. (1969). Ultrastructure and distribution of neuronal and glial elements on the motoneurone surface in the lumbosacral spinal cord of the cat. *Acta physiologica scandinavica, Suppl.* **332**, 5–48.

CULL, R. F. (1975). Role of axonal transport in maintaining central synaptic connections. *Experimental Brain Research* **24**, 97–101.

DE DUVE, C. (1963). The lysosome concept. In *Lysosomes* (ed. A. V. S. de Reuck & M. P. Cameron), pp. 1–31. London: J. & A. Churchill Ltd.

ECCLES, J. C. & SHERRINGTON, C. S. (1930). Numbers and values of individual motor units examined in some muscles of the limb. *Proceedings of the Royal Society of London, B* **106**, 326–357.

EMONET-DÉNAND, F. & LAPORTE, Y. (1975). Proportion of muscle spindles supplied by skeletofusimotor axons (β-axons) in peroneus brevis muscle of the cat. *Journal of Neurophysiology* **38**, 1390–1394.

FEDORKO, L. (1982). Localisation of respiratory motoneurone pools in the cats' spinal cord. *Journal of Physiology* **332**, 28P.

HARRISON, P. J., HULTBORN, H., JANKOWSKA, E., KATZ, R., STORAI, B. & ZYTNICKI, D. (1984). Labelling of interneurons by retrograde transsynaptic transport of horseradish peroxidase from motoneurones in rats and cats. *Neuroscience Letters* **45**, 15–19.

HENNEMAN, E. & MENDELL, L. M. (1981). Functional organisation of motoneuron pools and its inputs. In *Handbook of Physiology*, sect. 1, vol. II, part 1 (ed. J. M. Brookhart & V. B. Mountcastle), pp. 423–507. Bethesda, Maryland: American Physiological Society.

HENNEMAN, E., SOMJEN, G. & CARPENTER, D. O. (1965). Functional significance of cell size in spinal motoneurons. *Journal of Neurophysiology* **28**, 560–580.

JEFFERYS, J. G. R. (1982). The vibroslice, a new vibrating-blade tissue slicer. *Journal of Physiology* **324**, 2P.

JOHNSON, I. P. (1983). Morphological correlates of altered protein synthesis: An ultrastructural analysis of axotomy and diphtheritic intoxication. Ph.D. thesis, University of London.

JOHNSON, I. P. (1985). Ultrastructure of gamma motoneurones in the cat thoracic spinal cord. *Journal of Physiology* **360**, 46P.

KUFFLER, S. W., HUNT, C. C. & QUILLIAM, J. P. (1951). Function of medullated nerve fibres in mammalian ventral roots: efferent spindle innervation. *Journal of Neurophysiology* **14**, 29–54.

LEKSELL, L. (1945). The action potential and excitatory effects of the small ventral root fibres to skeletal muscle. *Acta physiologica scandinavica* **10**, *Suppl.* 31.

MATTHEWS, P. B. C. (1972). *Mammalian Muscle Receptors and Their Central Actions.* London: Edward Arnold Ltd.

NOVIKOFF, A. B. (1967). Enzyme localisation and ultrastructure of neurons. In *The Neuron* (ed. H. Hydén), pp. 255–318. Amsterdam: Elsevier.

NOVIKOFF, A. B. & NOVIKOFF, P. M. (1977). Cytochemical contributions to differentiating GERL from the Golgi apparatus. *Histochemical Journal* **9**, 525–551.

NYBERG-HANSEN, R. (1965). Anatomical demonstration of γ-motoneurones in the cat's spinal cord. *Experimental Neurology* **13**, 71–81.

OSCULATI, F., GAZZANELLI, G., MARELLI, M., FRANCESCHINI, F., AMATI, S. & CINT, S. (1980). Critical appraisal of the technique of labelling neurons by retrograde transport of horseradish peroxidase. *Journal of Submicroscopic Cytology* **12**, 391–400.

PULLEN, A. H. & SEARS, T. A. (1978). Modification of 'C' synapses following partial deafferentation of thoracic motoneurons. *Brain Research* **145**, 141–146.

PULLEN, A. H. & SEARS, T. A. (1983). Trophism between C-type axon terminals and thoracic motoneurons in the cat. *Journal of Physiology* **337**, 373–388.

REXED, B. (1952). The cytoarchitectonic organisation of the spinal cord in the cat. *Journal of Comparative Neurology* **96**, 415–496.

ROMANES, G. J. (1964). The motor pools of the spinal cord. *Progress in Brain Research* **11**, 93–116.

ROMANOVICZ, D. K. & HANKER, J. S. (1977). Wafer embedding: specimen selection in electron microscopic cytochemistry with osmiophilic polymers. *Histochemical Journal* **9**, 317–327.

SCHADÉ, J. P. & VAN HARREVELD, A. (1961). Volume distribution of moto- and interneurones in the peroneus-tibialis neuron pool of the cat. *Journal of Comparative Neurology* **117**, 387–398.

SEARS, T. A. (1964*a*). The fibre calibre spectra of sensory and motor fibres in the intercostal nerves of the cat. *Journal of Physiology* **172**, 150–161.

SEARS, T. A. (1964*b*). Efferent discharges in alpha and fusimotor fibres of intercostal nerves of the cat. *Journal of Physiology* **174**, 295–315.

SPRAGUE, J. M. (1951). Motor and propriospinal cells in the thoracic and lumbar ventral horn of the rhesus monkey. *Journal of Comparative Neurology* **95**, 103–121.

STRICK, P. L., BURKE, R. E., KANDA, K., KIM, C. C. & WALMSLEY, B. (1976). Differences between alpha and gamma motoneurones labelled with horseradish peroxidase by retrograde transport. *Brain Research* **113**, 582–588.

ULFHAKE, B. & CULLHEIM, S. (1981). Quantitative light microscopic study of the dendrites of cat spinal γ-motoneurones after intracellular staining with horseradish peroxidase. *Journal of Comparative Neurology* **202**, 585–596.

WESTBURY, D. R. (1979). The morphology of four gamma motoneurones examined by horseradish peroxidase histochemistry. *Journal of Physiology* **292**, 25–26P.

WESTBURY, D. R. (1982). A comparison of the structures of α- and γ-motoneurones of the cat. *Journal of Physiology* **325**, 79–91.

ADDENDUM

An ultrastructural description of the synaptic organisation of cat lumbosacral gamma motoneurons (Lagerbäck, P-Å, 1985, *Journal of Comparative Neurology* **240**, 256–264) was published after submission of this paper. It reports similar findings.